Computational investigation on the effects of main fuel injection timing on RCCI diesel engine combustion

Habtamu Deresso[*1], Venkata Ramayya[2], Ramesh Babu Nallamothu[1], Getachew Alemayehu[1]

[1]Department of Mechanical Engineering, Adama Science and Technology University, Adama, Ethiopia;
[2] Department of Mechanical Engineering, Jimma University Institute of Technology, Jimma, Ethiopia; and

E-Mail: simboo2400@gmail.com, venkata9999@yahoo.com, rbnallamothu@gmail.com, getachew.alemayehu@astu.edu.et

ABSTRACT

Self-contained energy sources of diesel engines are the power plants that provide mechanical power for pumps, off-road machinery, electrical power generation, agricultural tractors, ships, and the majority of transportation-related power generation. It comes in a variety of sizes, from a few hundred to thousands of horsepower. The IC Engine has proven to be critical to human social order in a variety of applications. Even though CI engines are more efficient than SI engines due to their ability to operate at a greater compression ratio, a leaner charge, and lower throttle losses; it has higher PM and nitrogen oxide emissions. The start of fuel injection is one parameter in developed RCCI operations for controlling emissions, in-cylinder charge reactivity as well as combustion phasing. Advancing the SOI timing has the optimum pressure and temperature; Maximum cylinder pressure and temperature take place at the baseline SOI Timing and low Cylinder pressure and temperature are found at retarded Start of Injection. The inspiring outcome of this combustion method is that it can be directly controlled using SOI timing which is impossible with most other LTC concepts. The heat release rate at retarded SOI is maximum, minimum at advanced and baseline SOI which generally indicates that the retard injection timing has more HRR and in advanced and optimum SOI is minimum. PM, NOx/100, CO_2/1000 and SE/10 are 0.334, 39.9, 0.917, and 0.682 g/kWh respectively are minimum at the retarded SOI and NOx, CO_2, and SE (0.345, 1.162, and 0.965 g/kWh respectively) are maximum at the standard SOI, however; PM is maximum (0.545 g/kWh) at advanced start of injection. In-cylinder combustion shows the maximum cylinder-pressure 147.6 bar at the optimum start of injection and minimum cylinder temperature of 1959.4K at the retarded SOI, and ringing intensity is minimum (4.49) MW/m^2 and maximum ignition delay (17.2) combustion duration at ASO.

1. Introduction

Internal combustion diesel engines are self-contained energy sources that provide mechanical power for pumps, off-road machinery, electrical power generation, agricultural tractors, ships, and the majority of transportation-related power generations. It come in a variety of sizes, from a few hundred to thousands of horsepower. The IC Engine has proven to be critical to human social order in a variety of applications. Compression ignition engines are generally more efficient than spark ignition engines due to their ability to operate at a greater compression ratio, a leaner charge, and lower throttle losses. The disadvantage of CI engines is their higher soot and nitrogen oxide emissions. Vehicles are subject to rigorous pollution and fuel efficiency requirements under current and future legislation(Splitter et al., 2010). These issues demanded the development of advanced engine technology as well as alternative to fossil fuels that are both efficient and emit minimal emissions(Mofijur et al., 2019). Several innovative CI combustion techniques have been investigating to reduce emissions in a cylinder while retaining higher thermal efficiency(Jacobs et al., 2017)(Kokjohn et al., 2010). To address future demands for cleaner and efficient power plant, majority of current techniques are classified as low-temperature combustion engines(Bhargava and Micklow, 2016)(Sharma et al., 2016)(Singh Juneja and Singh Sandhu, 2019)**.** In comparison to standard injection time, advance injection timing had a longer delay period, a higher cylinder peak pressure, a higher maximum heat release rate, and a shorter combustion duration. The combined effect of sophisticated fuel injection timing and exhaust gas recirculation on combustion characteristics was investigated, and it was discovered that with less combustion in the engine, high CPP, HMHRR, and shorter combustion duration can be achieved, as well as NOx and smoke emissions can be controlled simultaneously. Because slowing the pressure rise rate lowers the end-of-compression temperature, the late injection strategy has a significant impact on the heat release processes. Different EGR rates are compared to in-cylinder pressure and heat release rate. The increased EGR rate can cause a substantial delay in ignition and a reduction in peak pressure. EGR's thermodynamic and diluting effects account for this. Due to their high heat capacities, CO_2 and H_2O in the cylinder will absorb a lot of heat during the compression process, resulting in a lower in-cylinder temperature. Additionally, the diluting effect increases the global equivalence ratio,

Table 2: Engine Specifications

Make/Model	Kubota EA330-E4-NB1
No of Cylinder	1
Engine	4-stroke
Bore*Stroke	77.0 mm* 70.0 mm
Engine displacement	0.325L
Speed	1900 rpm
Connecting rod Length	124mm
Crank radius	35mm
Compression Ratio	24

which lowers the temperature [19][20]. The three-dimensional computational grids seen is a 60-degree sector mesh comprised of approximately 231, 024 Node at BDC. The various physical sub models CFD mesh grid is shown in the Fig.1.
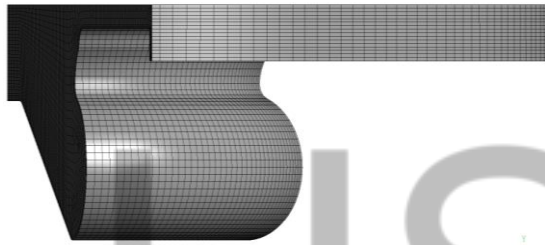
Figure 1 CFD mesh grids of the engine part geometry from CIV to OEV.

Table.1 Models used

Turbulence	RNG $k - \varepsilon$
Spray break-up	TAB
Spray Collision	O'Rourke
Combustion model	CHEMKIN Reduced
Fuel chemistry	Reduced PRF mechanism
NOx mechanism	Extended Zeldovich

The continuity equation for species m and energy equation in terms of specific internal energy are formulated in KIVA as given in Eqns. (1) and (2), respectively

$$\frac{\partial \rho_m}{\partial t} + \nabla.(\rho_m u) = \nabla.\left[\rho D \nabla \left(\frac{\rho_m}{\rho} \right) \right] + \rho_m^c + \rho^s \delta_{ml}....(1)$$

$$\frac{\partial (\rho I)}{\partial t} + \nabla.(\rho u I) = -P\nabla.u + (1 - A_{tkesw})^\sigma :$$

$$\nabla u - \nabla.J + A_{tkesw}\rho\varepsilon + \dot{Q}^C + \dot{Q}^s ....(2)$$

(Amsden, 1997), (Kakaee et al., 2015).

Where $\dot{Q}_m^c$ in Eq. (1) and $\dot{Q}^c$ in Eq. (2) are the source terms that need to be calculated by CHEMKIN codes(Kakaee et

al., 2015). Mathematical descriptions of these terms are as follows:

$$\dot{Q}_m^c = \rho \frac{dY_m}{dt}.................................... (3)$$

Where Y_m is the mass fraction of species m.

To calculate the molar production rate of chemical species participated in the chemical kinetics mechanism, the gas phase kinetics library of CHEMKIN-II (Kee et al., 1989) is integrated into KIVA code as shown in Fig. 2. In this procedure, the chemistry routine in the KIVA has been modified to perform chemistry solutions by iterative calling of DVODE (Brown et al., 1989). This new unit acts as an interface between KIVA and CHEMKIN and updates the combustion source terms of Eqs. (1) and (2). The binary linking file including species and chemical reactions data in CHEMKIN format is generated by CHEMKIN interpreter prior to each simulation. The KIVA code provides the species concentrations and thermodynamic information of each individual cell at every time step to pass to CHEMKIN solver (when the temperature rises above 600 K). The CHEMKIN subroutines construct M-set of stiff ordinary differential equations and DVODE subroutine is then successively called to compute the species net production rates at the end of each time step.

2. Computational modeling and simulation
2.1. Engine modeling

CATIA stands for computer-aided 3-D interactive application, which is a leading 3-D software tool utilized in most of the industries from automobile, and aerospace fields. So that, it is used to design the engine and piston with the right dimensions/specification which is the same size with the experiment's engine to use in the computational study to be validate comparatively.

2.2 3D-CFD Models
The governing equations in ANSYS ICE engine Fluent adopts mainly the equation of momentum, continuity, and energy to resolve the issues of computational fluid dynamics. Three-dimensional-CFD framework for simulations of reactive fluid flow is used. Hence, each computational cell can be treated as a homogeneously mixed reactor at each time-step. The 3D CFD Combustion simulation was used to simulate from closed intake valve to open exhaust valve. The governing equations are conservation of mass, momentum, energy, chemical components and the equation of state. Then, the in-cylinder pressure was used to calculate the HRR of EGB-Diesel dual

fuel engine. Usually, the HRR can be calculated according to the mass and energy conservation equations:

$$\frac{dQ_E}{d\varphi} = \frac{dU}{d\varphi} + \frac{dW}{d\varphi} + \frac{dQ_W}{d\varphi} \quad\text{........................(4)}$$

Where:

$\frac{dQ_E}{d\varphi}$ - represents the HRR; $\frac{dU}{d\varphi}$ -is the change of thermal energy of working medium; $\frac{dW}{d\varphi}$ - is the instantaneous expansion work and $\frac{dQW}{d\varphi}$ - is the instantaneous heat transfer loss through chamber wall. For the sake of calculation, Formula (4) can be changed into the following form by combining gas state equation:

$$\frac{dQ_E}{d\varphi} = \left[\frac{1}{\gamma-1}\left(V\frac{dP}{d\varphi} + \gamma p \frac{dV}{d\varphi}\right) - \frac{pv}{(\gamma-1)^2}\frac{d\gamma}{d\varphi} \right] + hA(T-T_W)...(5)$$

Where, γ is the ratio of specific heat; V is the chamber volume; p is the in-cylinder pressure; h is the heat transfer coefficient, which can be obtained according to Woschni equation; A is the chamber surface area; T is the mean gas temperature; T_W is the mean wall temperature. The calculated results of HRR are shown in Fig.3.

As illustrated, the HRR of GEB-diesel dual fuel engine exhibits one peak obviously like the HRR of GEB engine for all cases. In addition, a larger number and wider space distribution of ignition kernel are produced. As a result, the flame propagation of GEB initial combustion is enhanced and the proportion of premixed combustion increases. When the SOC is after TDC, the mixture burns during the expansion process, thus the highest combustion temperature as well as the peak HRR is influenced(Shu et al., 2018).

The engine size used was a single-cylinder light-duty, water cooled diesel engine modified to RCCI with the detail engine specifications and operating conditions shown in **Table 2.** The study was to reduce the NOx and PM while the thermal efficiency is higher using ANSYS Software CFD combustion simulation forecast result and validate with experimental results of 0.325L engine, compression ratio of 24, 4-stroke at AASTU (Addis Ababa Science and Technology University). The experiment took place in a modified CDC engine to RCCI engine to use PFI of the blended gasoline-ethanol in to the intake manifold and directly injection of diesel fuel in to the cylinder at about an ends of compression strokes. The injector was equipped with the hole diameter of 0.127 mm and at an angle of 70 degree, and injection pressure 137.3 bar can be provided. For the injection of gasoline and ethanol blends in the intake port injection pressure of 3.5 bar were mounted. In the experiments, wide ranges of operating conditions were tested for both diesel/gasoline-ethanol blends RCCI combustion. The start of injection (SOI) timing for diesel, EGR rate, and the engine load.

2.1 Model validation

Comparisons of cylinder pressure; Cylinder-temperature; AHRR; Emissions intensity in between the predictions and measurements are shown. The cylinder pressure of the experiment and simulations is as shown in Fig.2
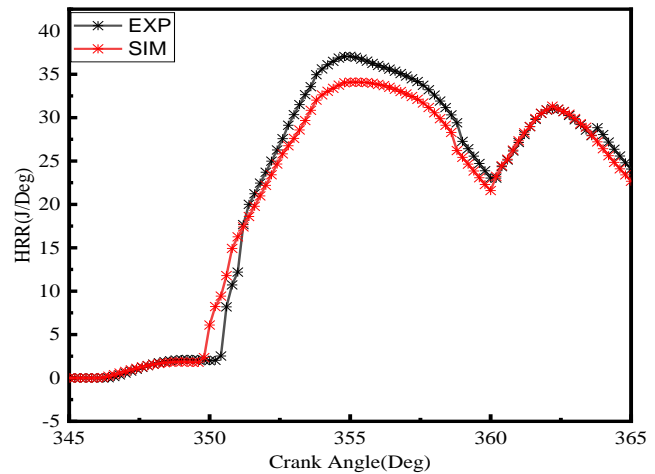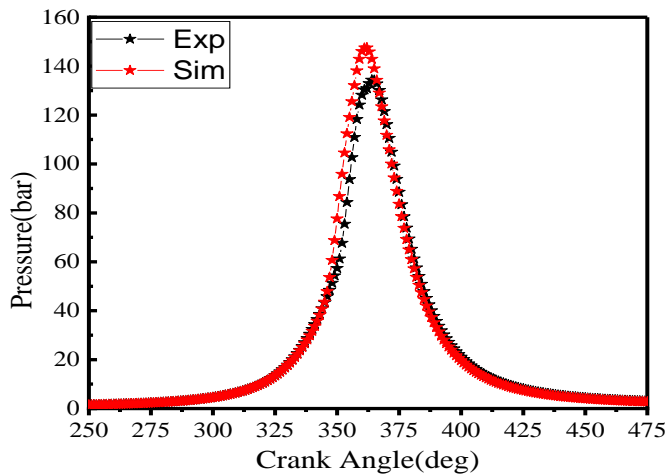
Figure 2 In-cylinder pressure and HRR result of the experiment & simulations

The detailed operating parameters for each case are listed in **Table 1, 2, 3 and 4**. In the simulations, variations in injection timing were achieved by perturbing the initial in-cylinder temperature at IVC. The logics of the diesel engine shows that the delaying DI fuel injection timing will result in poor fuel mixing and incomplete combustion. As can be

seen, the ASOI BTDC has the highest GIE and combustion efficiency, with maximum efficiency respectively, as well as the lowest emissions when compared to the other examples. The different result in HRR is as shown in the Fig.3. To minimize the PRR, optimized RCCI operation conditions frequently require the aid of EGR, especially at high load. As can be seen, raising the EGR rate reduced the PPRR. Additionally, NOx and soot emissions were lowered. Because of the dilution and heating impacts of EGR, the low-combustion temperature in the cylinder is responsible for the lower NOx and soot levels.

Table 3: Diesel fuel Properties

Diesel fuel Properties	
Density at 15℃	0.840
90% Volume recovered, ℃	342
FBP in Fuel Temperature, ℃	380
Total Sulfur, % wt	0.002
Flash point, PMCC, ℃	66
LHV in MJ/KG	42.5
IBP, ℃	38
Kinematics viscosity @ 40℃	3.5
Cloud point ℃	Max +5
Cetane index	48

Table 4: Basic Gasoline and ethanol fuel Properties

Gasoline fuel Properties		Basic Ethanol fuel Properties	
Density at 15℃	0.720-0.740	Chemical formula	C_2H_5OH
10% Volume recovered, ℃	74	Molecular weight	46
50% Volume recovered, ℃	80-127	LHV(MJ/kg)	26.8
90% Volume recovered, ℃	Max 190	Density at 15℃	0.79
FBP, ℃	Max 225	Boiling point (℃ @ 1atm)	78
Residue	Max 2	Flash point (℃ @ 1atm)	13
RON	Min 92	Auto ignition temperature(℃)	420
Total Sulfur, % wt	Max 0.05	Latent heat of vaporization (KJ/kg)	904
Reid Vapor pressure, KPa	41-65	Reid Vapor pressure, KPa	17
Existence gum, mg/100ml	Max 4	ON-RON	106
Doctor test	Negative	ON-MON	89

3. Result and Discussions
3.1. Effects of Injection Timing

Reactivity control compression Ignition in the study is the advanced low-Temperature Combustion engine using gasoline-ethanol blends of LRF fuels as a Port Fuel Injections and diesel as HRF of Direct Injection, respectively to reduce NOx and PM. The majority of the RCCI studies used conventional fossil fuels. The next generation of internal combustion engines, however, will almost certainly require fuel diversity due to future oil supply shortages. The effects of Injection Timing on performance and

emission were investigated at 30°, 25°, and 20° SOI timing. Advanced, optimum, and retarded SOI BTDC with a step of 5°crank angle in all simulations and experimental results are studied and validate through comparations. Accordingly, advancing the SOI timing before the top dead center has the optimum pressure and temperature (OCPT); Maximum cylinder pressure and temperature (MCPT) is takes place at the optimum SOI Timing and lower Cylinder pressure and temperature (LCPT) is found at retarded Start of Injection BTDC. So that, according to this study cylinder temperature and pressure is directly proportional as shown in the Fig.4 and 5.
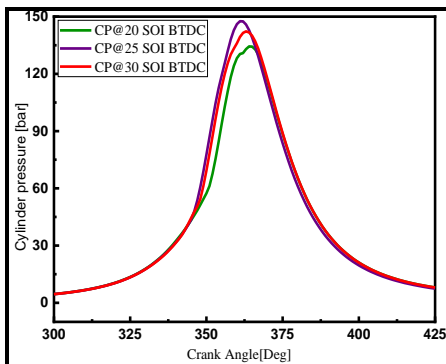

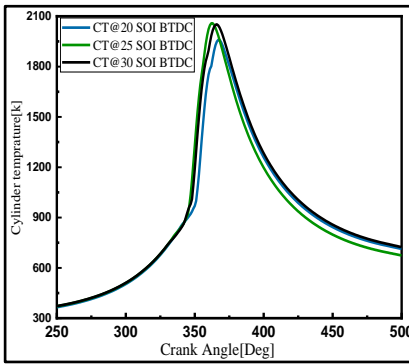Figure 3 In cylinder pressure[bar]
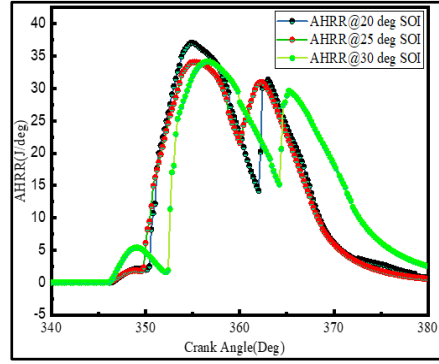

Figure 4 In cylinder Temperatures[K]

Figure 5 The HRR)[J/Deg]

The heat release rate (HRR) is affected as the start of injection timing varying in 5°-degree intervals from 20° to 30° before top dead center. **Fig.6** shows the maximum quantity of heat release rate at retarded start of injections before top dead center is maximum, and the heat release rate (HRR) is minimum at the advanced and optimum soi before

top dead center which generally indicates that the retard injection timing has more heat release rate and in advanced and optimum start of injections is minimum. The great issues as the world in the cases of diesel engine is that maximum production of the harmful NO_2 and PM emission due to the higher operating temperature of the engines. The emission investigation of soot and NOx production in the study is by using DISEL-RK Modeling that is developed by the Buman Technical University of Russia. So that; the SOI effect had tried to be seen. According to the result, NOx emission is maximum at baseline and advanced and minimum at the RSOI as shown in **Fig.7** and the maximum soot emission is at 20 and 30deg SOI BTDC and has a minimum value at 25deg SOI before TDC as shown in **Figure. 8**. The ecological effects of PM and NOx is minimum respectively at the retarded 0.334 and 39.9 g/kWh when retarded and maximum (1162 g/kWh) CO_2 at baseline start of injection but maximum summer emission 9.65 g/kWh at 25deg Start of Injection.
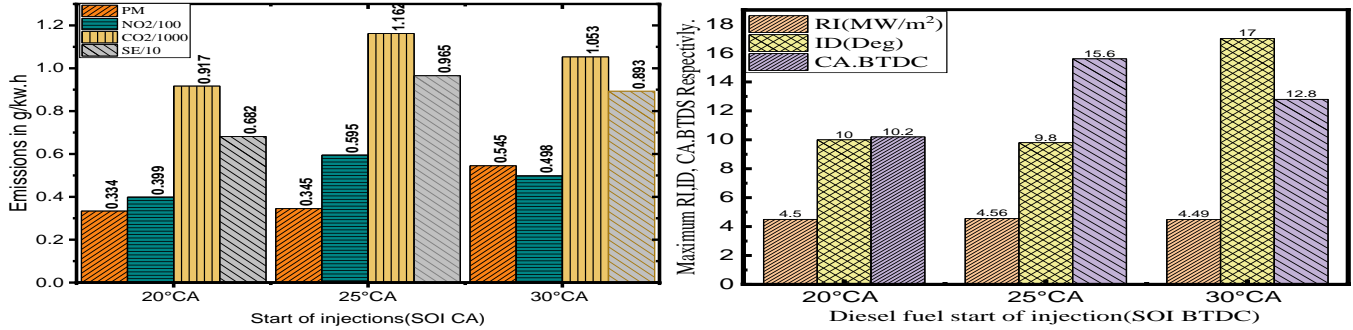

Figure 6 Emissions in different SOI and RI, ID and crank angle BTDC

The start of injection has a maximum mechanical and indicated efficiency (0.78, 0.40) at the retarded stage of injection respectively, and a maximum indicated mean effective pressure(6.3bar); minimum specific fuel consumption 0.28 kg/kWh; maximum brake power 2.43KW at a retarded start of injection and maximum brake torque 11.9 Nm at advanced start of injection. In-cylinder combustion shows the maximum cylinder-pressure 147.6bar at the baseline start of injection and minimum cylinder temperature 1959.4K at the retarded SOI; and ringing intensity is low 4.49 MW/m² and maximum injection pressure 1385.4 bar; and maximum ignition delay 17.2deg combustion duration 57.3°CA at ASOI.

$$RI \approx \frac{1}{2\gamma} \cdot \frac{\left(0.05 \cdot \left(\frac{dp}{dt}\right)_{max}\right)^2}{P_{max}} \cdot \sqrt{\gamma R T_{max}}$$
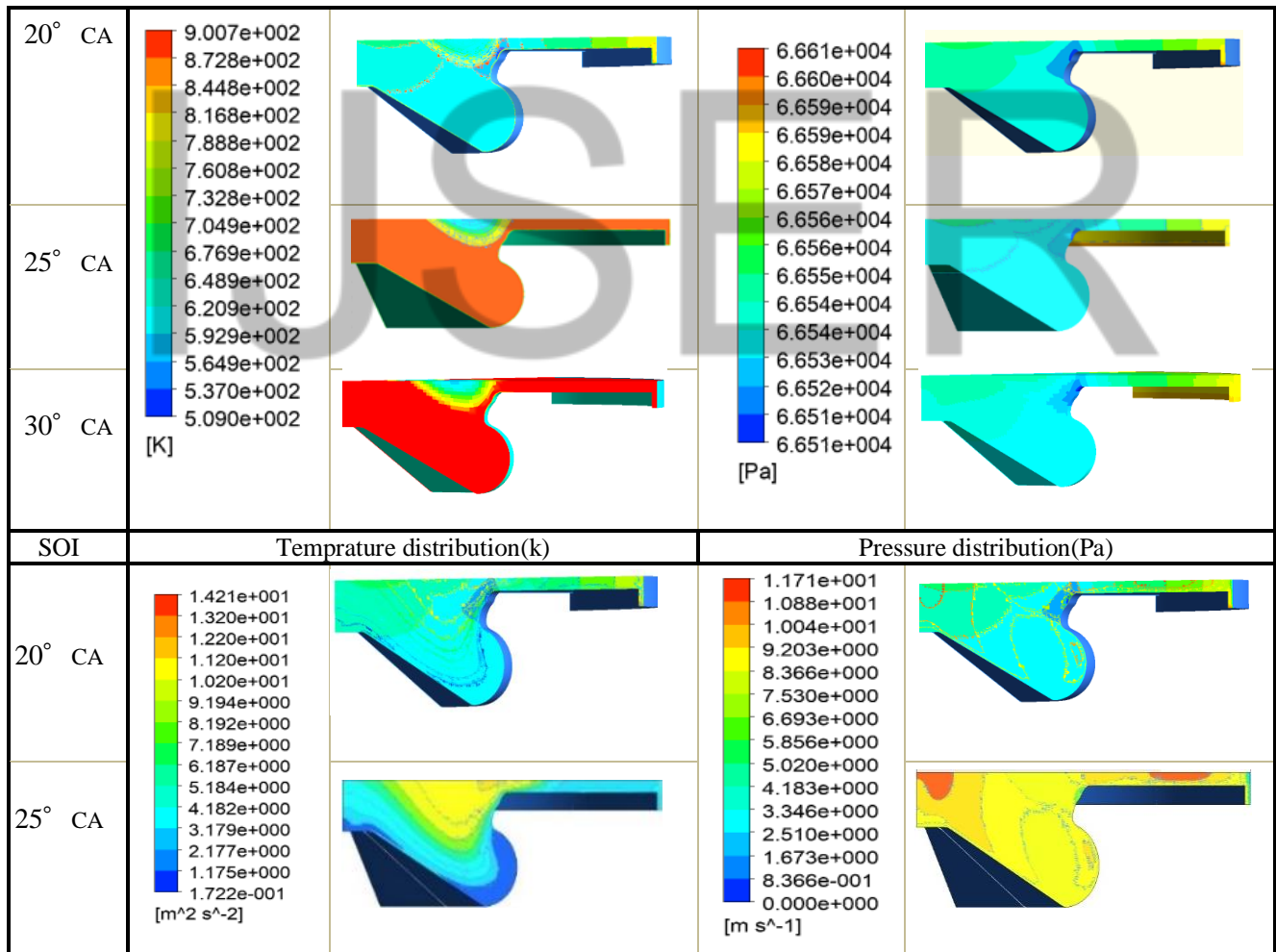
Where $(dp/dt)_{max}$ is the maximum pressure rise rate, P_{max} is the maximum cylinder pressure, R is the ideal gas constant, T_{max} is the global maximum temperature in cylinder, γ is the ratio of specific heat.
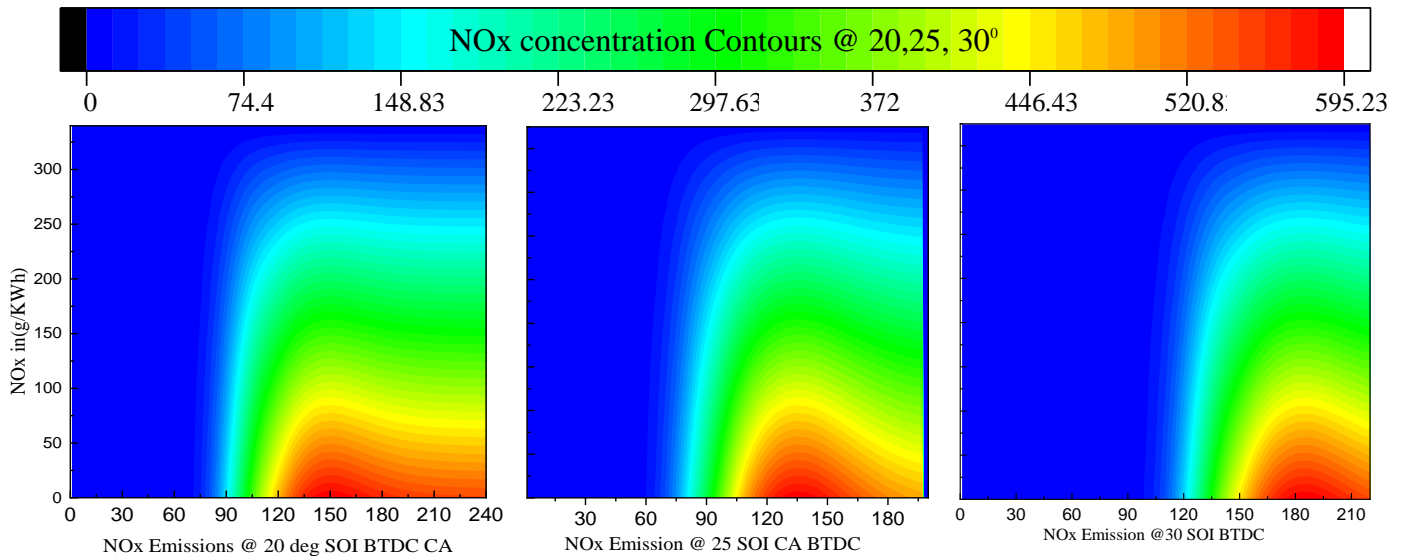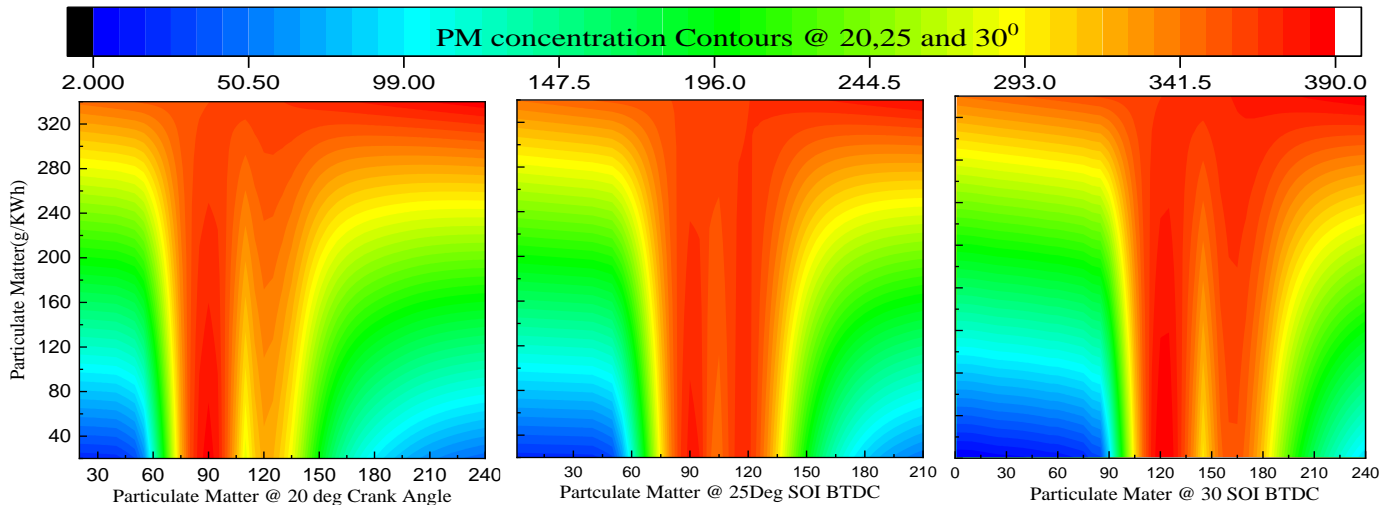
Figure 7 NOx and PM Contour plot diagrams

The contour plot of the ANSYS combustion simulation result as shown in the Figure 9 Below shows
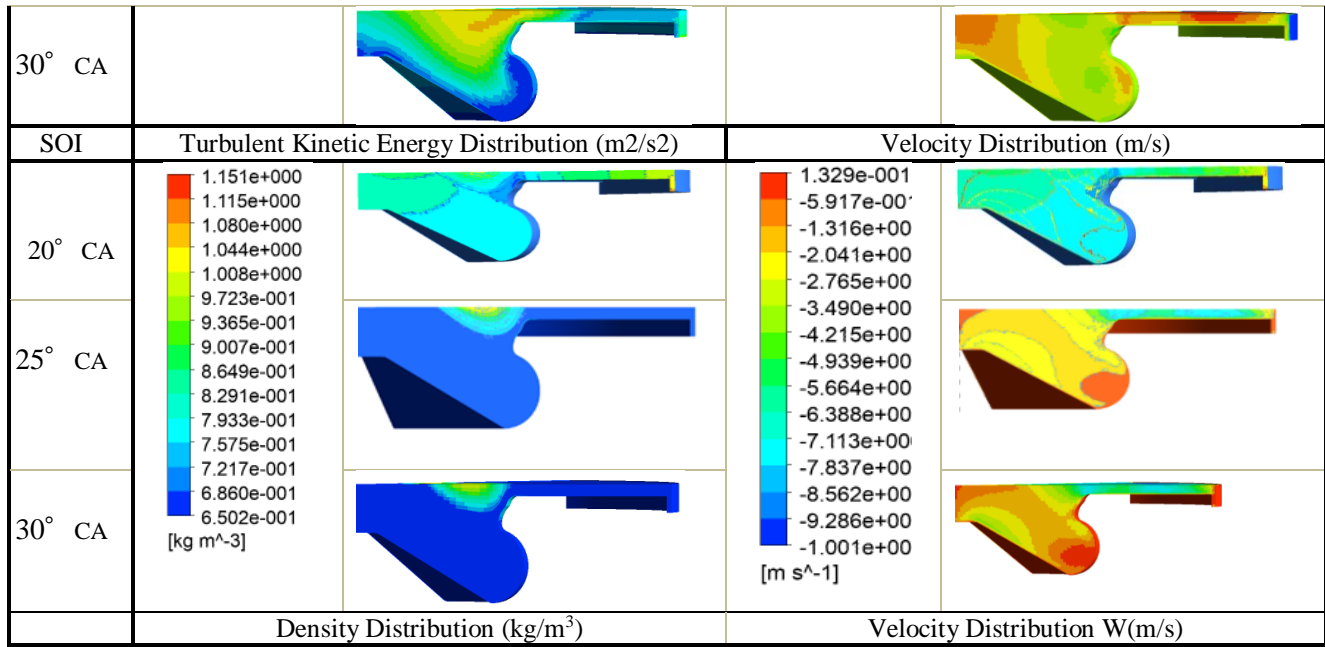
Figure 9 CFD Temperature, Pressure, TKE, Velocity, and Density contour distributions

Table.1 Single and Dual-fuel RCCI Engine

Authors Years	Parameter			Results						
	Parameters (SOI)	CP	HRR	RI	GIE	NOx	Soot	UHC	CO
(Mohammadian et al., 2020)	As ←SOI→	↑↓	↑↓	↓ – ↑	↑↓	↓↑	↓↑	↓↑	↓↑
	As IP↑	↓	↓	↓↑	↑	↓	↓	↑ @ max IP	↓
	As SCA↓	↑↑	↑↑	↑	↑↓↑	↑	↓↑↓	↓	↓↑↓
Flavio et al.,2017 (Chuahy and Ridge, 2017)	↑H₂ fuel Fraction&EGR	-	-	↑& ↑	↓	↓↓& ↓↓	↓↓ & ↓↓	↓&↓	↓&↓
(Poorghasemi et al., 2017)	Increasing PR of NG	-	↓	↓		↓	↓	↑	↑
	Retarding SOI2	↓	-	↑	↑	↓	↓	↑	↑
	Narrower SAs(Richer)	-	-	-	-	↑	↑	↑	↑
(Y. Li et al., 2013)	SOI	-	↓	↓	↑	↓	↓	-	-
(Zheng et al., 2018)	Loads, SOI retarded	-	-	-	↑	↓	↓	↓	↓
Authors Years	**Parameters (Loads)**	**CP**	**HRR**	**RI**	**GIE**	**NOx**	**Soot**	**UHC**	**CO**
(Y. Li et al., 2013)		-	↓	-	↑	↓	↓	-	-
(Curran et al., 2012)	Low loads CDC	↓	↓ at 2600rpm	-	↓	↑	↑	↓	↓
	Low loads RCCI	↑	↑ at 2600rpm	-	↓	↓	↓	↑	↑
	High loads CDC	↓	↓ at 2600rpm	-	↑	↑	↑	↓	↓
	High loads RCCI	↑	↑ at 2600rpm	-	↑	↓↓	↓	↑	↑
(Kaddatz et al., 2012)	Load at 5.5 bar (D-G)		↓	-	↑↑	↓		↑	↓	↓
	E10+EHN/E10		↑	-	↓	↑	↓	↑	↑
(Wang et al., 2016)	Low load	-	-	-	-	↓	↓	↑	↑
(Molina et al., 2015)	Load(Low)S	-	-	-	-	↓	↓	↑	↑
	Medium- load	↑	-	-	↑	↓	↓	↑	↑
	High load- MCP	↑↑	-	-	↑↑	↓	↓	↑	↑
(Pan et al., 2020)	Low Load(G-D)	-	-	-	-	↓	↓	↑	↓
	Low Load(B-D)	-	-k	-	↑	↓↓	↓↓	↑	↓↓

Where: ↑-increase, ↓-decrease, ← -advanced SOI, → - Retarded SOI, IP-injection pressure, SCA- Spray cone angle, DI- direct injection.

4. Conclusions

The benefit of the RCCI engine operation mode is that it minimizes the shortcomings of the CDC maximum release of NOx and PM and improves the emission, performance and combustion compared to the other LTC engine modes.

According to the investigations, the following conclusions are shown below:

Advancing the SOI timing has the optimum pressure and temperature; Maximum cylinder pressure and temperature take place at the baseline SOI Timing and low Cylinder

pressure and temperature are found at retarded Start of Injection.

₪ The inspiring outcome of the combustion is that it can be directly controlled using SOI timing which is impossible with most other LTC concepts.

₪ The heat release rate at retarded SOI is maximum, minimum at advanced and baseline SOI which generally indicates that the retard injection timing has more HRR and in advanced and optimum SOI is minimum.

₪ PM, NOx/100, CO_2/1000 and SE/10 are 0.334, 39.9, 0.917, and 0.682 g/kWh respectively are minimum at the retarded SOI and NOx, CO_2, and SE (0.345, 1.162, and 0.965 g/kWh respectively) are maximum at the standard SOI, however; PM is maximum (0.545 g/kWh) at advanced start of injection.

₪ In-cylinder combustion shows the maximum cylinder-pressure 147.6 bar at the optimum start of injection and minimum cylinder temperature of 1959.4K at the retarded SOI, and ringing intensity is minimum (4.49) MW/m^2 and maximum ignition delay (17.2) combustion duration at ASOI.

References

Akihama, K., Takatori, Y., Inagaki, K., Sasaki, S., and Dean, A. M. (2001). Mechanism of the smokeless rich diesel combustion by reducing temperature. *SAE Technical Papers*, *2001*(724). https://doi.org/10.4271/2001-01-0655

Bhargava, A., and Micklow, G. J. (2016). *Study of Characteristics of Low Temperature Combustion (LTC) Study of Characteristics of Low Temperature Combustion (LTC). November.*

Chuahy, F., and Ridge, O. (2017). *Single fuel RCCI combustion using reformed fuel. April.*

Curran, S. J., Hanson, R. M., and Wagner, R. M. (2012). Reactivity controlled compression ignition combustion on a multi-cylinder light-duty diesel engine. *International Journal of Engine Research*, *13*(3), 216–225. https://doi.org/10.1177/1468087412442324

Ho, R. J., Kumaran, P., and Yusoff, M. Z. (2016). Development of High Efficiency and Low Emission Low Temperature Combustion Diesel Engine with Direct EGR Injection. *IOP Conference Series: Earth and Environmental Science*, *32*(1), 0–5. https://doi.org/10.1088/1755-1315/32/1/012016

Jacobs, T. J., Committee, C., Caton, J. A., and Holtzapple, M. T. (2017). *A HIGH EFFICIENCY AND CLEAN COMBUSTION STRATEGY FOR COMPRESSION IGNITION ENGINES: INTEGRATION OF LOW HEAT. August.*

Kaddatz, J., Andrie, M., Reitz, R., and Kokjohn, S. (2012). Light-duty reactivity controlled compression ignition combustion using a cetane improver. *SAE Technical Papers*. https://doi.org/10.4271/2012-01-1110

Kakaee, A. H., Rahnama, P., and Paykani, A. (2015). CFD Study of Reactivity Controlled Compression Ignition (RCCI) combustion in a heavy-duty diesel engine. *Periodica Polytechnica Transportation Engineering*, *43*(4), 177–183. https://doi.org/10.3311/PPtr.7756

Kokjohn, S. L., Hanson, R. M., Splitter, D. A., and Reitz, R. D. (2010). Experiments and modeling of dual-fuel HCCI and PCCI combustion using in-cylinder fuel blending. *SAE International Journal of Engines*, *2*(2), 24–39. https://doi.org/10.4271/2009-01-2647

Li, J., Yang, W. M., An, H., and Zhao, D. (2015). Effects of fuel ratio and injection timing on gasoline/biodiesel fueled RCCI engine: A modeling study. *Applied Energy*, *155*, 59–67. https://doi.org/10.1016/j.apenergy.2015.05.114

Li, Y., Jia, M., Liu, Y., and Xie, M. (2013). Numerical study on the combustion and emission characteristics of a methanol/diesel reactivity controlled compression ignition (RCCI) engine. *Applied Energy*, *106*(x), 184–197. https://doi.org/10.1016/j.apenergy.2013.01.058

Li, Y., Jia, M., Xu, L., and Bai, X. (2020). Multiple-objective optimization of methanol / diesel dual-fuel engine at low loads : A comparison of reactivity controlled compression ignition (RCCI) and direct dual fuel stratification (DDFS) strategies. *Fuel*, *262*(November 2019), 116673. https://doi.org/10.1016/j.fuel.2019.116673

Mofijur, M., Hasan, M. M., Mahlia, T. M. I., Rahman, S. M. A., Silitonga, A. S., and Ong, H. C. (2019). Performance and emission parameters of homogeneous charge compression ignition (HCCI) engine: A review. *Energies*, *12*(18). https://doi.org/10.3390/en12183557

Mohammadian, A., Chehrmonavari, H., Kakaee, A., and Paykani, A. (2020). Effect of injection strategies on a single-fuel RCCI combustion fueled with isobutanol/isobutanol+DTBP blends. *Fuel*, *278*(April), 118219. https://doi.org/10.1016/j.fuel.2020.118219

Molina, S., García, A., Pastor, J. M., Belarte, E., and Balloul, I. (2015). Operating range extension of RCCI combustion concept from low to full load in a heavy-duty engine. *Applied Energy*, *143*, 211–227. https://doi.org/10.1016/j.apenergy.2015.01.035

Pan, S., Liu, X., Cai, K., Li, X., Han, W., and Li, B. (2020). Experimental study on combustion and emission characteristics of iso-butanol/diesel and gasoline/diesel RCCI in a heavy-duty engine under low loads. *Fuel*, *261*(October 2019), 116434. https://doi.org/10.1016/j.fuel.2019.116434

Poorghasemi, K., Saray, R. K., Ansari, E., Irdmousa, B. K., Shahbakhti, M., and Naber, J. D. (2017). Effect of diesel injection strategies on natural gas/diesel RCCI combustion characteristics in a light duty diesel engine. *Applied Energy*, *199*, 430–446. https://doi.org/10.1016/j.apenergy.2017.05.011

Sharma, T. K., Rao, G. A. P., and Murthy, K. M. (2016). Homogeneous charge compression ignition (HCCI) engines: A review. *Archives of Computational Methods in Engineering*, *23*(4), 623–657. https://doi.org/10.1007/s11831-015-9153-0

Shu, J., Fu, J., Liu, J., Zhang, L., and Zhao, Z. (2018).

Experimental and computational study on the effects of injection timing on thermodynamics, combustion and emission characteristics of a natural gas (NG)-diesel dual fuel engine at low speed and low load. *Energy Conversion and Management*, *160*(October 2017), 426–438. https://doi.org/10.1016/j.enconman.2018.01.047

Singh Juneja, H., and Singh Sandhu, S. (2019). Experimental Investigation of PPCI Engine fuelled with Ethanol. *IOP Conference Series: Materials Science and Engineering*, *691*(1). https://doi.org/10.1088/1757-899X/691/1/012059

Splitter, D., Reitz, R., and Hanson, R. (2010). High efficiency, low emissions RCCI combustion by use of a fuel additive. *SAE Technical Papers*, *3*(2), 742–756. https://doi.org/10.4271/2010-01-2167

Wang, Y., Yao, M., Li, T., Zhang, W., and Zheng, Z. (2016). A parametric study for enabling reactivity controlled compression ignition (RCCI) operation in diesel engines at various engine loads. *Applied Energy*, *175*, 389–402. https://doi.org/10.1016/j.apenergy.2016.04.095

Yousefi, A., Birouk, M., and Guo, H. (2020). On the Variation of the Effect of Natural Gas Fraction on Dual-Fuel Combustion of Diesel Engine Under Low-to-High Load Conditions. *Frontiers in Mechanical Engineering*, *6*(November). https://doi.org/10.3389/fmech.2020.555136

Zheng, Z., Xia, M., Liu, H., Shang, R., Ma, G., and Yao, M. (2018). Experimental study on combustion and emissions of n-butanol/biodiesel under both blended fuel mode and dual fuel RCCI mode. *Fuel*, *226*(March), 240–251. https://doi.org/10.1016/j.fuel.2018.03.151